

# Geometrical, electronic and magnetic properties of $\text{Na}_{0.5}\text{CoO}_2$ from first principles

Zhenyu Li, Jinlong Yang,\* J.G. Hou, and Qingshi Zhu  
*Hefei National Laboratory for Physical Sciences at Microscale,  
Laboratory of Bond Selective Chemistry,  
and Structure Research Laboratory,  
University of Science and Technology of China, Hefei, Anhui 230026, P.R. China*

(Dated: May 23, 2019)

## Abstract

We report a first-principles projector augmented wave (PAW) study on  $\text{Na}_{0.5}\text{CoO}_2$ . With the sodium ion ordered insulating phase being identified in experiments, pure density functional calculations fail to predict an insulating ground state. When the on-site Coulomb interaction is included by an additional Hubbard parameter  $U$ , charge ordered insulating ground state can be obtained. The electronic structures for different  $U$  are generally different. At a moderate value of  $U$  (4.0 eV for example), the ground state is antiferromagnetic, with a  $\text{Co}^{4+}$  magnetic moment about  $1.0 \mu_B$  and a magnetic energy 0.12 eV/Co. The rehybridization process is studied in the DFT+U point of view.

PACS numbers: 71.28.+d, 71.27.+a, 75.25.+z

arXiv:cond-mat/0403727v1 [cond-mat.mtrl-sci] 30 Mar 2004

## I. INTRODUCTION

$\text{Na}_x\text{CoO}_2$  was originally studied as a kind of rechargeable battery material<sup>1</sup> and thermoelectric material<sup>2,3,4</sup>. More recently, the discovery of the superconductivity in its hydrated  $x=0.35$  composition<sup>5</sup>, with the effect of hydration being found to be limited to lattice expansion<sup>6,7</sup>, make it receive a renewed interest.  $\text{Na}_x\text{CoO}_2$  has a crystal structure consisting of 2D triangular lattice Co sheets, octahedrally coordinated with O above and below the Co planes, and layers of Na ions sandwiched between the  $\text{CoO}_2$  sheets. The phase diagram of  $\text{Na}_x\text{CoO}_2$  has been determined by changing the Na content  $x$  using a series of chemical reactions<sup>8</sup>. Their electronic and magnetic properties are found to be strongly dependent on the number of charge carriers introduced by deviations from stoichiometry in the Na sublattice.

Theoretical studies on the electronic structure of  $\text{Na}_x\text{CoO}_2$  are very active. The early work by Singh<sup>9,10</sup> focused on the magnetic properties. He predicted a weak instabilities of itinerant ferromagnetic character in range  $x=0.3$  to  $x=0.7$ , with competing but weaker itinerant antiferromagnetic solution. Virtual crystal approximation was used, instead of supercell, for the partially occupation of Na sites. As a result, the possibility of sodium ion and  $\text{Co}^{3+}/\text{Co}^{4+}$  charge ordering is not allowed. Using pseudopotential plane wave method, Ni *et al.*<sup>11</sup> have optimized the geometries for  $\text{Na}_x\text{CoO}_2$  ( $x = 0.25, 0.5, 0.75$  and  $x = 1$ ) with a  $2 \times 2 \times 1$  supercell. They found that the itinerant ferromagnetism is strongly suppressed by the local distortions of the oxygen around the cobalt. With optimized geometries, they identified a phase transition from wide-band ferromagnetic to narrow band paramagnetic metals with varying  $x$ . By carefully examining the doped electron density, Marianetti *et al.*<sup>6</sup> found that the rigid band model is not suitable for this Na doped system. A rehybridization driven by a competition between the on-site Coulomb interaction and the  $e_g$ -oxygen hybridization is identified. They have also used a modified Hubbard model to study this kind of rehybridization. Within the framework of density functional theory (DFT), the on-site Coulomb correlation effects can be dealt with DFT+U method<sup>12</sup>. Zou *et al.*<sup>13</sup> have studied the electronic structure of  $\text{Na}_x\text{CoO}_2$  with varying  $c/a$  ratio using DFT+U method. They did not find critical change from DFT result of the band structure near  $E_F$ , except a notable decrease of the DOS at  $E_F$ . To consider the relations between correlation and charge ordering, Pickett and coauthors<sup>14,15</sup> have applied the DFT+U method to a  $\sqrt{3} \times \sqrt{3} \times \frac{1}{2}$

supercell of  $\text{Na}_x\text{CoO}_2$  at  $x = 1/3$  and  $x = 2/3$ . They found that the parameter  $U$  is critical to charge and spin ordering (in small supercell, their charge disproportionation always leads to  $\text{Co}^{3+}/\text{Co}^{4+}$  charge ordering). They suggested that the phase diagram of  $\text{Na}_x\text{CoO}_2$  is characterized by a crossover from effective single-band character with  $U \gg W$  for  $x > 0.5$  into a three-band regime for  $x < 0.5$ , where  $U \sim W$  and correlation effects are substantially reduced.

$\text{Na}_{0.5}\text{CoO}_2$  is of special interests among the  $\text{Na}_x\text{CoO}_2$  family. In the recent experimental phase diagram, a novel sodium ion ordered insulating state at  $x = 0.5$  was found<sup>8</sup>, with notable superstructure<sup>16,17</sup>. This insulating state separates two kinds of metallic phase, *i.e.* Curie-Weiss metal for  $x > 0.5$  and paramagnetic metal for  $x < 0.5$ . It is suggested that the occurrence of the insulating state indicates a strong interaction between the ions and holes even though they occupy separate layers, and a charge ordering is thought to accompany the sodium ion ordering<sup>8</sup>. Therefore it is interesting to compare the electronic structure based on this experimental sodium ion ordered structure with previous theoretical results. On the other hand, the correlation effects of  $\text{Na}_{0.5}\text{CoO}_2$  is considered to be a betweenness comparing to the small values for  $x > 0.5$  and relatively large values for  $x < 0.5$ <sup>11,15</sup>, which demands a study at the DFT+U level in addition to adopting experimental superstructure. Unfortunately, there is not such a theoretical work in the literature. In this paper, we report the electronic structure of  $\text{Na}_{0.5}\text{CoO}_2$  considering both the possibility of charge ordering and the effects of correlation.

## II. COMPUTATIONAL METHOD

The calculations in this work were performed with the Vienna *Ab initio* Simulation Package (VASP)<sup>18,19</sup>, which is a first-principles plane-wave code, treating the exchange and correlation in the DFT scheme. In this study, the Perdew-Wang functional form<sup>20</sup> of generalized gradient approximation (GGA) was used. For spin-polarized calculations, the spin interpolation of Vosko *et al.*<sup>21</sup> was also adopted. The projector augmented wave (PAW)<sup>22</sup> method in its implementation of Kresse and Joubert<sup>23</sup> was used to describe the electron-ion interaction. The Kohn-Sham equations were solved via a Davidson-block iteration scheme<sup>18</sup>.

A  $\sqrt{3} \times 2 \times 1$  supercell was introduced to describe the experimental sodium ion ordering. Brillouin zone (BZ) integrations were performed on a well converged grid of  $8 \times 8 \times 4$

Monkhorst-Pack<sup>24</sup> special points. The total energy and density of states (DOS) were calculated using the linear tetrahedron method with Blochl corrections. The plane wave kinetic energy cutoff was fixed to 500 eV. Dudarev *et al.*'s approach<sup>25</sup> was adopted for DFT+U calculations. Since this DFT+U functional depends only on the difference of Hubbard parameter  $U$  and screened exchange parameter  $J$ ,  $J$  was kept fixed to 1 eV during all DFT+U calculations. Geometry relaxation is performed at the spin unpolarized GGA level.

### III. RESULTS AND DISCUSSION

#### A. Geometrical properties

A  $\sqrt{3} \times 2 \times 1$  superstructure of  $\text{Na}_{0.5}\text{CoO}_2$  has been found by powder neutron diffraction experiment<sup>16</sup>. This superstructure has the  $Pnmm$  space group symmetry, with a cell formula:  $\text{Na}_4\text{Co}_8\text{O}_{16}$ . In this experimental structure model, the Na1 and Na2 sites ( $2b$  and  $2d$  Wyckoff sites for original  $P6_3/mmc$  space group, and  $2b$  and  $2a$  sites for this  $Pnmm$  space group respectively) are equally occupied, and the ordered Na ions form one-dimensional zigzag chains. Two types of Co ions ( $4f$  and  $4d$ ), which differ subtly in their coordination by oxygen, are also in chains. The existence of two kinds of Co site allow the emergence of two inequivalent Co ions, namely  $\text{Co}^{3+}$  and  $\text{Co}^{4+}$ , in the process of self-consistency. Therefore this structure model can be used to study the possibility of charge ordering.

The geometry optimization, starting from the experimental structure, reaches its convergence until all forces vanished within 0.01 eV/Å. The optimized geometry is shown in Fig. 1. During the optimization, the cell parameters are fixed to the experimental values ( $a = 4.876\text{Å}$  and  $c = 11.063\text{Å}$ ), which results in only a neglectable stress. Relaxations of atomic positions from the experimental start point are also found to be very small. In an ideal structure model of  $\text{Na}_x\text{CoO}_2$ , Co and O may form layers of edge-shared  $\text{CoO}_6$  octahedra in a triangular lattice, but distortion of the octahedra with the variation of the O height  $z_0$  from its ideal value is always exists in real system. Our optimized  $z_0$  varies from 0.0845  $c$  to 0.0892  $c$  for different O sites, resulting in the Co-O-Co angles varying from  $96.2^\circ$  to  $97.0^\circ$ . Comparing to the  $90^\circ$  angle in the undistorted octahedra, the optimized structure shows a considerable distortion of the oxygen octahedra. The corresponding distortion given by Ni *et al.*<sup>11</sup> for a  $2 \times 2 \times 1$  supercell is significantly larger than ours, but we get similar distortions

for both types of supercells by optimizations using VASP.

## B. GGA electronic structure

We can clearly identify three well separated manifolds in the paramagnetic GGA band structure and DOS of  $\text{Na}_{0.5}\text{CoO}_2$ , as shown in Fig. 2. The lowest in energy is the O  $2p$  bands, with a bandwidth about 5.5 eV (only part of them shown in the figure). The other two manifolds comes from the Co  $3d$  orbitals, which is splitted into a lower lying  $t_{2g}$  manifold and an upper lying  $e_g$  manifold, separated by approximately 2.5 eV according to the oxygen octahedral crystal field. Although these three manifolds are well separated in energy, the hybridizations of O  $2p$  states with both the  $t_{2g}$  and  $e_g$  states are notable. The Fermi energy locate at the upper edge of the  $t_{2g}$  manifold, indicating a metallic GGA ground state.

The low energy properties of  $\text{Na}_{0.5}\text{CoO}_2$  will be determined by the  $t_{2g}$  manifold, which has a bandwidth of 1.6 eV. The trigonal symmetry of the Co sites in the triangular  $\text{CoO}_2$  layer splits the  $t_{2g}$  states further into one with  $a_g$  symmetry and a doubly degenerate  $e'_g$  pair. In Fig. 2, we also plot the  $a_g$  (Co  $d_{z^2}$ ) partial DOS. As found by Lee *et al.*<sup>15</sup>, the  $a_g$  states have a bandwidth almost identical to that of the whole  $t_{2g}$  manifold, which indicates that the widely used single-band model may not sufficient to describe the GGA electronic structure of this material.

Fermiology often plays an important role in the electronic structure of materials. LDA/GGA band structure is expected to give valuable and accurate information about the Fermi surface even in system with strong correlations<sup>7</sup>. We calculate the Fermi surface in the  $k_z = 0$  plane with a  $32 \times 32 \times 1$  BZ sampling. The first BZ at the reciprocal lattice in the  $k_z = 0$  plane is plotted in Fig. 3a, together with the first BZ of the original hexagonal lattice. Due to band folding for superstructure, the Fermi surface become very complex. We notice that the band structure of the superstructure geometry is far from simply band folding, for example, the two original  $2/3 \Gamma - K$  pockets (see reference 9) merge together and form a new nesting big cylinder at the center of the new BZ.

Spin-polarized calculations are carried out in order to address the possibility of magnetic ordering. When the ordering is constrained to be ferromagnetic (FM), a stable low spin solution is obtained, with magnetic moments of 0.4 and 0.45  $\mu_B$  for Co1 and Co2 respectively. The corresponding energy gain from ferromagnetic instability is only 26 meV/Co. The

moment values are smaller than that ( $0.5 \mu_B$ ) reported by Singh<sup>9</sup> under virtual crystal approximation, which may due to the difference between their structural model and ours. In our structure, the triangular symmetry is slightly broken.

Although Antiferromagnetic (AFM) ordering is geometrically frustrated on the 2D triangular lattice, it is also possible to construct an AFM model in the sodium ion ordered phase, by altering the direct of the magnetic moments of neighboring Co2 atoms. The magnetic moments at Co1 site are constrained to zero by symmetry. Our AFM model results in a magnetic moments of Co ions about  $0.39 \mu_B$ , which is much larger the result ( $0.21 \mu_B$ ) for the Singh AFM model<sup>9</sup>. We notice that in that model each Co ion has also two nearest neighbors of like spin in addition to four of opposite spin.

Unitl now, we get an FM half-metallic GGA ground state. Comparing to the results of Singh<sup>9</sup>, we may conclude that the GGA electronic structure is not very sensitive to the ordering of sodium ions. Even with this experimental sodium ordered structure, no accompanied charge ordering is found in the FM ground state. In the AFM ordering state, where charge ordering is enforced, the magnetic energy ( $7 \text{ meV/Co}$ ) is much smaller than that of FM state, which indicates the enforced charge ordering under GGA level is unfavorable in energy. This result is consistent with the calculations for  $\text{Na}_{1/3}\text{CoO}_2$ , where attempts using LDA to obtain self-consistent AFM spin ordering always converge to the FM or nonmagnetic solution<sup>14</sup>. The discrepancy between theory and experimental observation of charge ordered insulating phase naturally lead to a further consideration of correlation effect.

### C. DFT+U electronic structure

DFT+U<sup>12,25</sup> is a kind of methods aiming to deal with the on-site Coulomb interaction within the framework of DFT. It treat the local electrons in a Hartree-Fock manner, which drives local orbital occupations to integral occupancy as  $U$  increases. For transition metal oxide, one may find a larger split of  $d$  orbitals for larger  $U$ , as shown in Fig. 4 and Fig. 5, where partial DOS of cobalt  $3d$  orbitals and oxygen  $2p$  orbitals are shown for FM and AFM ordering respectively. The cobalt  $3d$  partial DOS for Co1 and Co2 sites are separated.

In Fig. 4, the top panel is the GGA result, and the three below panels represent three typical electronic structure behaviors for different  $U$  values. For small  $U$  (see panel b), the electronic structure is similar to the above GGA one, except for a strong trend towards gap

opening and charge ordering. As shown in Fig. 6, the moments on the two inequivalent Co sites are nearly equal and also similar to the GGA values (which is the  $(U - J) \rightarrow 0$  limit) until  $U = U_c = 3$  eV. Above  $U_c$ , the unoccupied part of the  $a_g$  states weight more and more for Co2 states with the increase of  $U$ . Disproportionation from  $\text{Co}^{3.5+}$  into  $s = \frac{1}{2} \text{Co}^{4+}$  and  $s = 0 \text{Co}^{3+}$  ions is nearly complete at  $U = 4$  eV and is accompanied by a metal insulator (Mott-like) transition from conducting to insulating. This insulating phase results from the splitting of the  $a_g$  states, which lead to an unoccupied narrow band containing one hole for each Co2 ions and an occupied band on the Co1 ion, as shown in Fig. 4c. We notice that the charge ordering and gap opening with a moderate  $U$  is far from obvious, since Zou *et al.*<sup>13</sup> get an insulating ground state with a 5 eV Coulomb  $U$  but without any supercell adopted. Therefore the sodium ion ordering is critical to the insulating ground state.

There is no clear boundary for moderate and large values of  $U$ , but a relatively large  $U$  value will features several characters as shown in Fig. 4d. First, the empty  $a_g$  band are pushed further higher, which make it strongly mix with the upper  $e_g$  bands. Secondly, the large splitting of the Co  $3d$  orbitals even squeeze some Co2  $3d$  states to the bottom of the O  $2p$  manifold, and consequently the O  $2p$  character at the edge of valence band near Fermi energy has exceeded the Co  $3d$  characters. Thirdly, the magnetic moments of cobalt are exceed  $1 \mu_B$  in this region (up to  $1.42 \mu_B$  per Co for  $U = 7.0$  eV), which seems curious at first sight. We now give two possible rationalizations for this observation. One interpretation comes from the population analysis process. We notice that oxygen is also spin polarized in our calculations for large  $U$ , which makes the net magnetic moment is still about  $1.0 \mu_B$  per Co. Therefore the nominal magnetic moment being larger than  $1 \mu_B$  per Co may be just an artifact of PAW population analysis as a result of the strong hybridization between Co and O. Another possibility is that the large on-site Coulomb interaction may really promote a transition from low spin state to a intermediate spin state as demonstrated by Korotin *et al.*<sup>26</sup> for Co ions in vertex sharing  $\text{CoO}_6$  octahedra. This type of transition is consistent with the strong mixing of empty  $a_g$  and  $e_g$  bands.

The evolution of electronic structures with  $U$  for AFM ordering is generally similar to that for FM ordering. The most significant difference is that the charge ordering occurs well before gap opening. As shown in Fig. 6, the  $\text{Co}^{4+}$  moment grows immediately as  $U$  is increased from 1 eV. But the gap opens until  $U = 3$  eV, which is different from the results of Lee *et al.*<sup>15</sup> for  $\text{Na}_x\text{CoO}_2$  with  $x = 1/3$  and  $x = 2/3$ . The energy differences between the FM

and AFM phases are also dependent on the values of  $U$ . For small and large  $U$ , FM ordering is favorable in energy, and the AFM ordering is preferred for moderate  $U$ . Experiments support an AFM coupling in  $\text{Na}_x\text{CoO}_2$ <sup>27,28</sup>. As previously discussed, the lift of the AFM energy for small  $U$  is caused by the artificial charge ordering. For large  $U$ , the drop of FM energy may be a result of the deep DOS of the majority spin component as shown in Fig. 4d.

From Fig. 4 and Fig. 5, we can find an interesting splitting and ordering of the  $e_g$  orbitals. With the increase of  $U$ , the lower part of the  $e_g$  orbitals becomes mainly from Co1 sites and the upper part from Co2 sites. We notice that this kind of orbital ordering of unoccupied  $e_g$  orbitals will not affect the low energy properties of  $\text{Na}_{0.5}\text{CoO}_2$ . Although it has been found in  $\text{LaCoO}_3$ <sup>26</sup>, orbital ordering of valence band orbitals is not very possible in this structure, since they are not doubly degenerated.

A rehybridization process is proposed to describe the competition between the on-site Coulomb interaction and the  $e_g$ -oxygen hybridization in doped CoO layers<sup>6</sup>. This process can be seen clearly from the partial DOS of O  $2p$  orbitals as shown in Fig. 4 and Fig. 5. At GGA level, hybridization of oxygen  $2p$  states and  $e_g$  states are more significant than the  $t_{2g}$ -oxygen hybridization. With the increase of  $U$ , the on-site Coulomb interaction becomes stronger, which can be minimized by unmixing the oxygen and  $e_g$  orbitals in order to decrease the occupation of the  $e_g$  orbitals. In Fig. 4 and Fig. 5, we can clearly see this kind of unmixing by the decrease of oxygen  $2p$  partial DOS in the  $e_g$  manifold. For large value of  $U$ , the hybridization of oxygen  $2p$  states and  $t_{2g}$  states is somewhat enhanced, which is not included in the modified Hubbard model study by Marianetti *et al.*<sup>6</sup>.

As previously mentioned, different  $U$  leads to very different electronic structures. Therefore it is important to estimate the actual on-site Coulomb interaction strength in this kind of materials, of which very different values are proposed in the literature<sup>9,13,15,29</sup>.  $\text{Na}_{0.5}\text{CoO}_2$  is thought as a betweenness with moderate  $U$  value<sup>15</sup>, which is consistent with the following two experimental facts. First, the insulating ground state suggests that the value of  $U$  should not be too small. Secondly,  $\text{Na}_x\text{CoO}_2$  with  $x$  away from 0.5 is always metallic indicates a narrow energy gap for  $\text{Na}_{0.5}\text{CoO}_2$ , which prefer a not too large value of  $U$ . Since there were experimental report<sup>30</sup> on electron mass enhancement for small  $x$  of  $\text{Na}_x\text{CoO}_2$ , people have compared the experimental electronic specific heat coefficient  $\gamma$  with the band value to estimate the strength of correlation<sup>9,15</sup>. But in the  $\text{Na}_{0.5}\text{CoO}_2$  case, where Hubbard

type correlation drives system to a Mott insulator,  $\gamma$  will be reduced by the correlation effects. In fact, the experimental  $\gamma$  is only 3 mJ/mol-K<sup>2</sup>,<sup>16</sup> which is much smaller than our GGA band value (10.5 mJ/mol-K<sup>2</sup>).

At a plausible value of  $U$ , 4 eV for example, AFM coupling is favored over FM coupling with an energy difference 6.3 meV/Co, which is consistent with the negative Curie-Weiss temperature  $\theta$  in Na<sub>*x*</sub>CoO<sub>2</sub><sup>27,28</sup>. The AFM magnetic moment for Co<sup>2+</sup> is 1.0  $\mu_B$ .

#### IV. CONCLUSION

We have studied the geometrical, electronic and magnetic properties of Na<sub>0.5</sub>CoO<sub>2</sub> based on DFT+ $U$  method. Without including on-site Coulomb interaction  $U$ , the experimental insulating phase can not be produced by DFT. For small value of  $U$ , ground state is still metallic. At this time, no charge ordering occurs for FM coupling, and symmetry enforced charge ordering for AFM coupling is unfavorable in energy. Increase parameter  $U$  to a moderate value can open an energy gap and form charge ordering for both FM and AFM states. Large  $U$  value will largely split the Co 3*d* orbitals, which leads to squeezing Co 3*d* states to the bottom of O 2*p* manifold, mixing of empty  $a_g$  and  $e_g$  states, and large Co magnetic moments.

Accompany with the early work on Na<sub>*x*</sub>CoO<sub>2</sub> ( $x = 1/3$  and  $x = 2/3$ ), our study will obviously shed some insights into understanding of the complex interplay of Na content, superstructure, correlation effects and tendency of various type of ordering in Na<sub>*x*</sub>CoO<sub>2</sub>. While a complete understanding of this issue, for example, why the  $x = 2/3$  case with stronger commensurability effects and maybe also stronger correlation is not a charge ordered insulator, will need much further work.

#### Acknowledgments

This work is partially supported by the National Project for the Development of Key Fundamental Sciences in China (G1999075305, G2001CB3095), by the National Natural Science Foundation of China (50121202, 20025309, 10074058), by the Foundation of Ministry

of Education of China, and by ICTS, CAS.

---

- \* Corresponding author. E-mail: jlyang@ustc.edu.cn
- <sup>1</sup> C. Fouassier, C. Delmas, and P. Hagemmuller, *Mater. Res. Bull.* **10**, 443 (1975)
- <sup>2</sup> I. Teradaki, Y. Sasago, and K. Uchinokura, *Phys. Rev. B* **56**, 12685 (1997)
- <sup>3</sup> I. Teradaki, *Physica B* **328**, 63 (2003)
- <sup>4</sup> Y. Wang, N. S. Rogado, R. J. Cava and N. P. Ong, *Nature* **423**, 425 (2003)
- <sup>5</sup> K. Takada, H. Sakurai, E. Takayama-Muromachi, F. Izumi, R. A. Dilanian, and T. Sasaki, *Nature* **422**, 53 (2003)
- <sup>6</sup> C. A. Marianetti, G. Kotliar, and G. Ceder, arXiv:cond-mat/0312514.
- <sup>7</sup> M. D. Johannes and D. J. Singh, arXiv:cond-mat/0401646.
- <sup>8</sup> M. L. Foo, Y. Wang, S. Watauchi *et al.*, arXiv:cond-mat/0312174.
- <sup>9</sup> D. J. Singh, *Phys. Rev. B* **61**, 13397 (2000)
- <sup>10</sup> D. J. Singh, *Phys. Rev. B* **68**, 020503(R) (2003)
- <sup>11</sup> J. Ni and G.-M. Zhang, arXiv:cond-mat/0305423.
- <sup>12</sup> V. I. Anisimov, F. Aryasetiawan and A. I. Lichtenstein, *J. Phys.: Condens. Matter* **9** 767 (1997).
- <sup>13</sup> L.-J. Zou, J.-L. Wang and Z. Zeng, arXiv:cond-mat/0307560.
- <sup>14</sup> J. Kunes, K.-W. Lee, and W. E. Pickett, arXiv:cond-mat/0308388.
- <sup>15</sup> K.-W. Lee, J. Kunes, and W. E. Pickett, arXiv:cond-mat/0403018.
- <sup>16</sup> Q. Huang, M. L. Foo, J. W. Lynn *et al.*, arXiv:cond-mat/0402255.
- <sup>17</sup> H. W. Zandbergen, M. L. Foo, Q. Xu *et al.*, arXiv:cond-mat/0403206.
- <sup>18</sup> G. Kresse and J. Furthmuller, *Comput. Mater. Sci.* **6**, 15 (1996)
- <sup>19</sup> G. Kresse and J. Furthmuller, *Phys. Rev. B* **54**, 11169 (1996).
- <sup>20</sup> J.P. Perdew *et al.*, *Phys. Rev. B* **46**, 6671 (1992).
- <sup>21</sup> S. H. Vosko, L. Wilk and M. Nusair, *Can. J. Phys.* **58**, 1200 (1980)
- <sup>22</sup> P. E. Blochl, *Phys. Rev. B* **50**, 17953 (1994)
- <sup>23</sup> G. Kresse and D. Joubert, *Phys. Rev. B* **59**, 1758 (1996)
- <sup>24</sup> H.J. Monkhorst and J.D. Pack, *Phys. Rev. B* **13**, 5188 (1976).
- <sup>25</sup> S. L. Dudarev, G. A. Botton, S. Y. Savrasov *et al.*, *Phys. Rev. B* **57**, 1505 (1998)
- <sup>26</sup> M. A. Korotin, S. Yu. Ezhov, I. V. Solovyev *et al.*, *Phys. Rev. B* **54**, 5309 (1996)

- <sup>27</sup> H. Sakurai, K. Takada, S. Yoshii *et al.*, Phys. Rev. B **68**, 132506 (2003)
- <sup>28</sup> T. Fujimoto, G.-Q. Zheng, Y. Kitaoka *et al.*, Phys. Rev. Lett. **92**, 047004 (2003)
- <sup>29</sup> A. Chainani, T. Yokoya, Y. Takata *et al.*, arXiv:cond-mat/0312293.
- <sup>30</sup> F. C. Chou, J. H. Cho, P. A. Lee *et al.*, arXiv:cond-mat/0306659.

FIG. 1: The Optimized crystal structure of  $\text{Na}_{0.5}\text{CoO}_2$ . The designations of the Na and Co atoms are as indicated.

FIG. 2: GGA paramagnetic band structure (left panel) and density of states (DOS)(right panel) of  $\text{Na}_{0.5}\text{CoO}_2$ . The Fermi energy is at zero.  $\Gamma=(0,0,0)$ ,  $M=(1/2,0,0)$ ,  $N=(1/2,1/2,0)$ , and  $A=(0,0,1/2)$ . The dot line in the DOS panel represents the Co  $a_g$  partial DOS.

FIG. 3: (a) First Brillouin zone for the original  $P6_3/mmc$  lattice (blue) and the superstructure lattice (red). (b) Fermi surface of  $\text{Na}_{0.5}\text{CoO}_2$  within the first Brillouin zone in the  $k_z = 0$  plane.

FIG. 4: Ferromagnetic density of states (DOS). Total DOS is in black. Red and blue lines for  $3d$  partial DOS of Co1 and Co2 respectively. Green lines is the O  $2p$  partial DOS. (a) GGA result and  $U =$  (b) 3.0, (c) 4.0, and (d) 7.0 eV results are presented.

FIG. 5: Antiferromagnetic density of states (DOS). Total DOS is in black. Red and blue lines for  $3d$  partial DOS of Co1 and Co2 respectively. Green lines is the O  $2p$  partial DOS. (a) GGA result and  $U =$  (b) 3.0, (c) 4.0, and (d) 7.0 eV results are presented..

FIG. 6: Effect of the intraatomic repulsion  $U$  on the (a) magnetic moments and (b) energy gap of  $\text{Na}_{0.5}\text{CoO}_2$  for ferromagnetic order (black) and antiferromagnetic order (red). In the magnetic moment plotting, empty points indicate Co1 values and filled points indicate Co2 values.

Figure 1, Li *et al.*



Figure 2, Li *et al.*

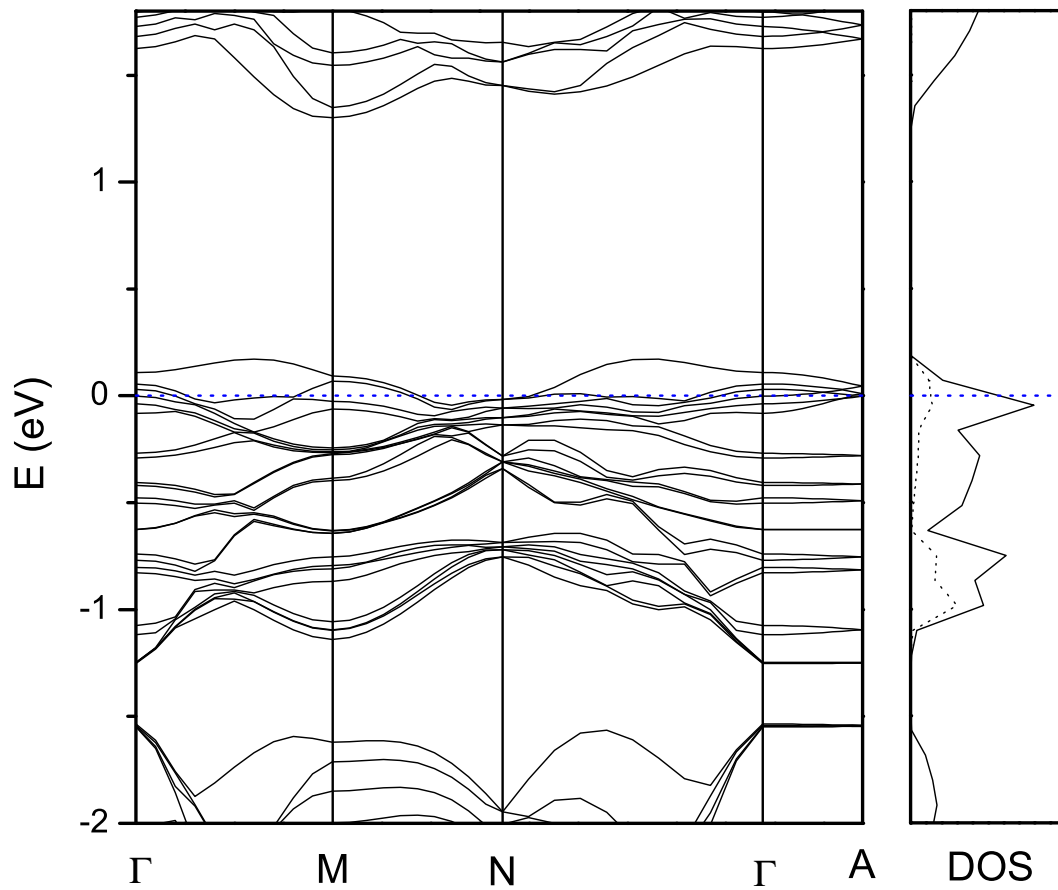


Figure 3, Li *et al.*

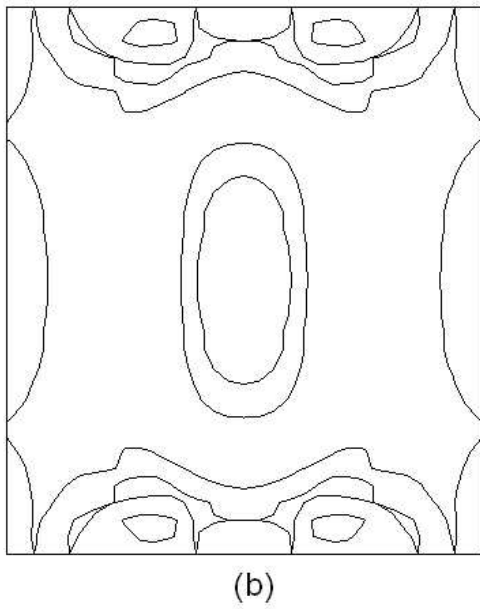
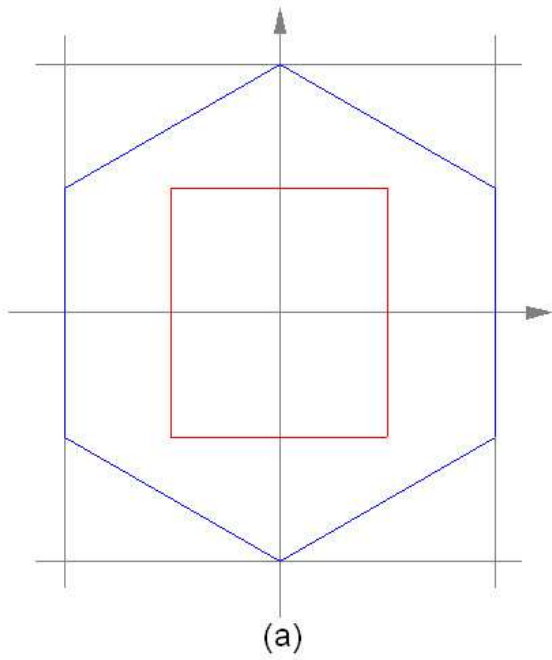


Figure 4, Li *et al.*

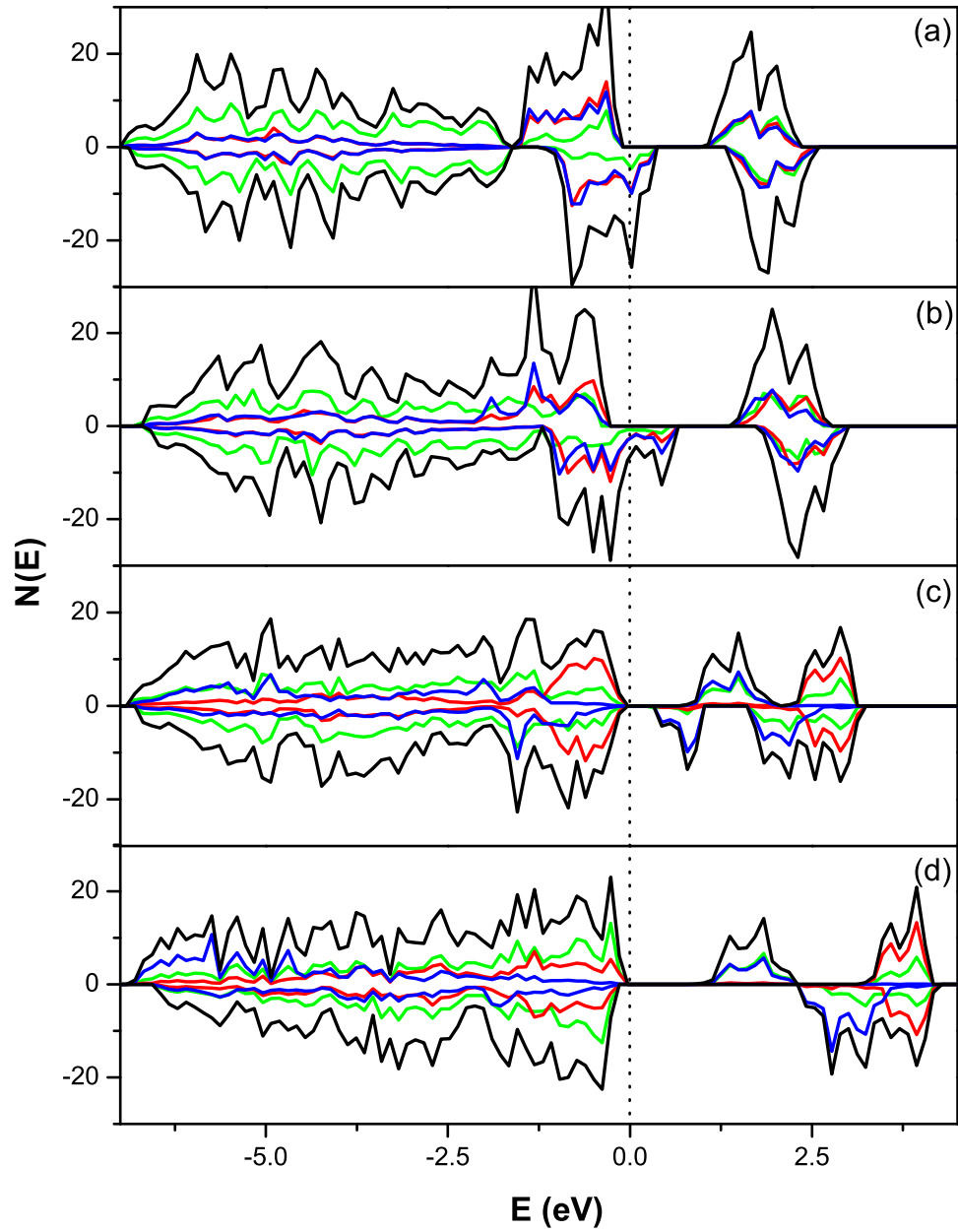


Figure 5, Li *et al.*

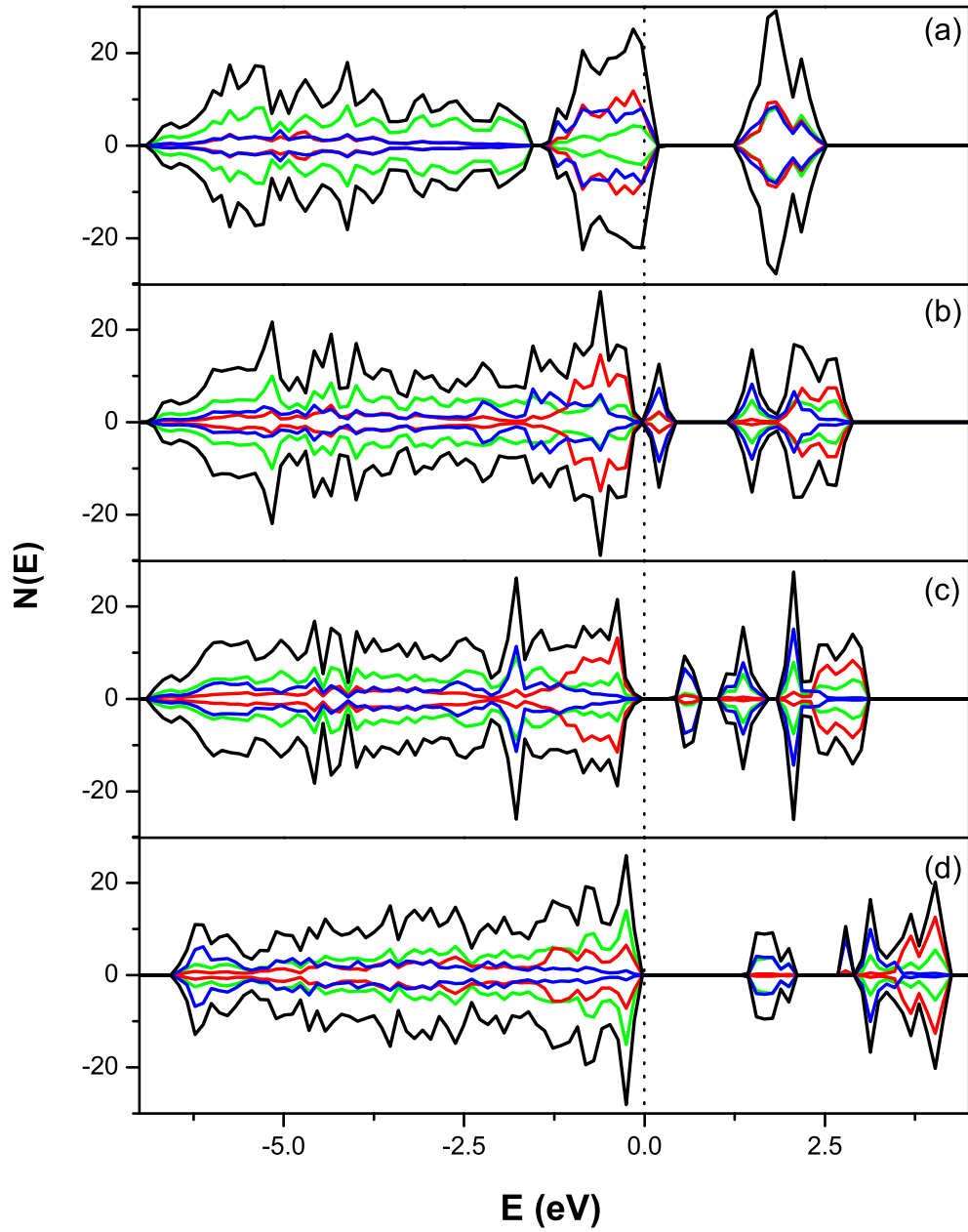


Figure 6, Li *et al.*

